Electronic Supplementary Material (ESI) for Journal of Materials Chemistry A.
This journal is © The Royal Society of Chemistry 2019

Supporting Information

Thermo-Osmotic Energy Conversion and Conservation by Nanochannels

Kexin Chen[†,a], Lina Yao[†,a], Fei Yan[b], Shanshan Liu[a], Rongjie Yang[a] and Bin Su[a]*

a. Institute of Analytical Chemistry, Department of Chemistry, Zhejiang University, Hangzhou 310058, China
b. Department of Chemistry, Zhejiang Sci-Tech University, 928 Second Avenue, Xiasha Higher Education Zone, Hangzhou 310018, China

Table of Contents

S1. Materials and Reagents

All chemicals and reagents were used as received without further purification. All aqueous solutions were prepared with ultrapure water (18.2 MΩ cm). Tetraethoxysilane (TEOS, ≥ 99.0%), cetyltrimethylammonium bromide (CTAB, ≥ 98%), poly(methyl methacrylate) (PMMA, Mw = 996000) were purchased from Sigma-Aldrich. Potassium chloride (KCl, AR) and sodium chloride (NaCl, AR) were bought from Sinopharm Chemical Reagent.

ITO coated glass (surface resistivity < 17 ohm/square, thickness 100 ± 20 nm) was ordered from Zhuhai Kaivo (Zhuhai, China). Prior to use, ITO was treated with 1 M NaOH solution, and then sonicated in acetone, ethanol, and deionized water sequentially. Ion-tracked PET membrane (12 m in thickness; ion-track density: 10^8 cm^{-2}) was purchased from Wuwei Kejin Xinfa Co. Ltd.

S2. Measurements and Characterizations

Transmission electron microscopy (TEM, HT7700, Hitachi) and scanning electron microscopy (SEM, SU-8010 field-emission scanning electron microscope, Hitachi) were employed to characterize the morphology and structures of SNC/PET hybrid nanochannels. Ionic current measurement was carried out with Keithley 6847 picoammeter (Keithley Instruments, Cleveland). A pair of Ag/AgCl electrodes were used to supply voltage and measure the current.

The thermoelectric response was recorded by a custom-made setup. Briefly, a micro ceramic heater (Zhuhai Huiyou Electronics, China) was employed to regulate the temperature of one solution. A DC power (QJ6003S, Ningbo Jiuyuan Electronics, China) was connected to the heater to control the heating rate and temperature range. A pair of temperature microsensors (PT100, Tenghui Wenkong Instruments, China) were immersed in two solutions to measure the instantaneous temperature. The temperature and its change were real-time recorded and stored with a temperature sensor (THMA temperature recorder, Tenghui Wenkong Instruments, China). The measurement accuracy and working range of the temperature sensor are ± 0.15 K and −173.15 − 533.15 K, respectively. The trans-nanochannel potential was synchronously collected by an Autolab electrochemical workstation (PGSTAT302N, Metrohm) using two Ag/AgCl electrodes. The time resolutions of temperature recorder and trans-nanochannel potential are 1 s and 0.25 s, respectively.

S3. Preparation of SNC/PET Hybrid Nanochannels

Preparation of SNC Membrane. SNC was firstly grown on the ITO glass using the Stöber-solution growth approach.[S1] Briefly, the bare ITO glasses were immersed in the precursor solution containing 70 mL water, 30 mL ethanol, 0.16 g CTAB, 10 μL concentrated ammonia aqueous solution and 80 μL TEOS. After 24 h under the quiescent condition at 60 °C, SNC with CTAB micelles confined in silica nanochannels was formed on the ITO surface (namely CTAB@SNC/ITO), and then aged at 100 °C overnight. The CTAB micelles in the silica nanochannels were removed by immersing the CTAB@SNC/ITO in 0.1 M HCl ethanol solution for 15 min under stirring to obtain micelle-free electrode (namely SNC/ITO).

Preparation of PET with Conical Nanochannels. Poly(ethylene terephalate) membrane (PET, thickness: 12 μm, pore density: 10^8 pores cm^{-2}), irradiated with heavy ions, was treated by UV light (at 254 nm) for 1 h before etching. The PET membrane was subsequently chemically etched from one side by 9 M NaOH solution, whereas the other side was put in contact with stopping solution containing 1 M KCl and 1 M HCOOH as neutralization agents. The etching process was performed at about 303 K and the trans-membrane ionic current at voltage of 1 V was monitored. The etching was stopped when an obvious current increase was observed.

Preparation of SNC/PET Hybrid Nanochannels. SNC/PET hybrid nanochannels membrane was prepared using the PMMA-assisted transfer approach as previously reported.[S2] Briefly, PMMA solution (3.5% wt in anisole) was spin-coated on the top surface of SNC/ITO at 2000 rpm for 30 s. After solvent evaporation at room temperature for 1 h and heating at 115 °C for 15 min, the obtained PMMA protected SNC/ITO was treated with 2 M HCl to etch the ITO layer and the free-standing PMMA/SNC was obtained. Subsequently, a piece of PET membrane with conical nanochannels was used as the substrate to fish out the free-standing PMMA/SNC. Finally, the top PMMA layer was dissolved in the mixture of toluene and acetone (V/V

= 10/1) for 24 h to obtain the hybrid nanochannel membrane with perforated channels. The morphology structure of SNC/PET is illustrated in **Figure 1**.

EDS analysis of PET membrane and SNC/PET membrane. In order to further confirm the cross-section structure of SNC/PET membrane, we did energy dispersive x-ray analysis (EDS) as an assisted proof. **Figure S1a**, **c** shows the top-view SEM images of PET and SNC/PET membranes, in which the square areas were scanned for EDS analysis. As displayed in **Figure S1b**, Si element was barely detected for bare PET membrane. In contrast, in **Figure S1d**, an obvious amount of Si element can be detected for SNC/PET one, indicating the attachment of SNC to PET.

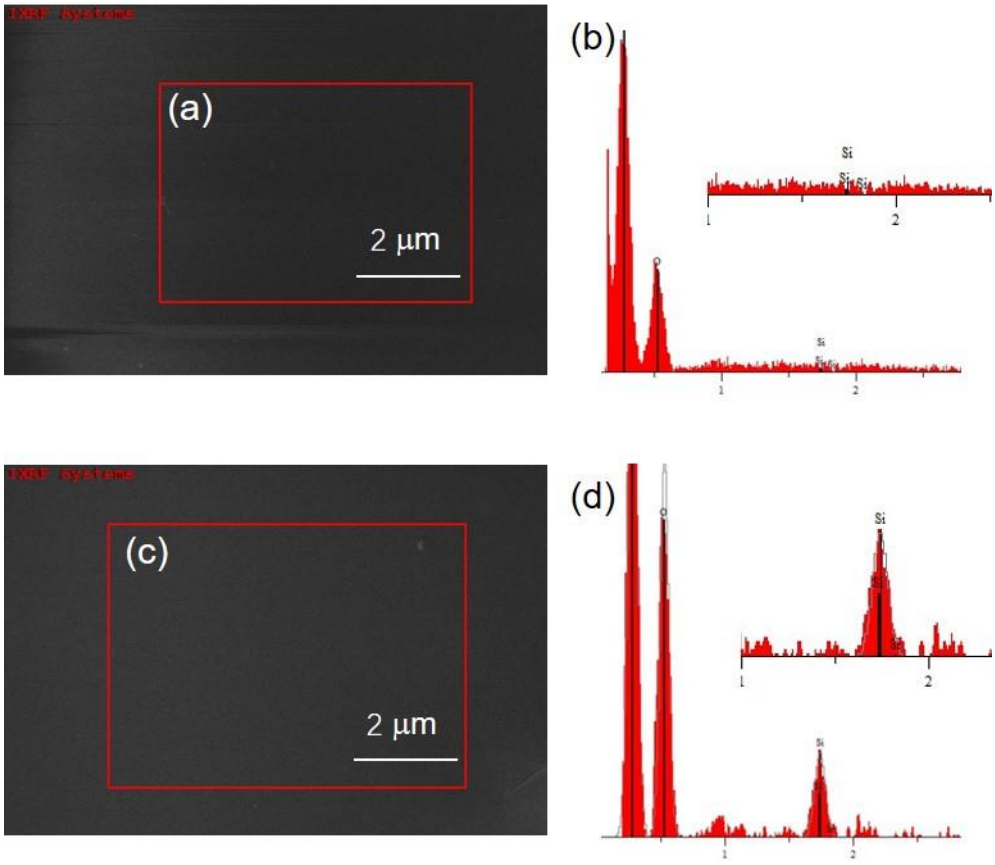

Figure S1. Top-view SEM images of PET membrane (a) and SNC/PET membrane (c) and the corresponding EDS analysis.

S4. *I-V* Responses of Nanochannels

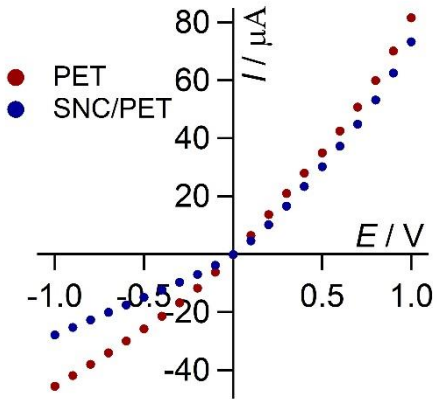

Figure S2. Comparison of *I-V* responses of PET conical nanochannels (red) and SNC/PET hybrid nanochannels (blue) in 10 mM KCl.

Figure S2 compares the current-voltage (*I-V*) characteristic of PET conical nanochannels and SNC/PET hybrid nanochannels in 10 mM KCl. Apparently, an enhanced ionic current rectification was observed, with the rectification ratio ($|I_{+1.0\ V}/I_{-1.0\ V}|$) increased from 1.9 to 2.6, confirming the successful preparation of layered nanochannel structure. Moreover, the ionic current did not decrease drastically (from 81.6 μA to 73.3 μA at +1.0 V) after SNC was adhered to PET nanochannels, indicating that silica nanochannels have a negligible effect on the ion permeability thanks to its high pore density.

S5. *I-V* Responses of Nanochannels under Salinity Gradient

To study the performance of energy conversion by SNC/PET hybrid nanochannels. We investigated the *I-V* responses of SNC/PET under a salinity gradient (0.5 M/0.01 M NaCl). From blue line in **Figure S3**, the salinity gradient is from SNC to PET (namely $c_{b\text{-}PET}/c_{b\text{-}SNC}$ = 0.01 M/0.5 M), V_{oc} and I_{sc} obtained are 162.8 mV and 20.1 μA, respectively. Whereas under reversed salinity gradient from PET to SNC (namely $c_{b\text{-}PET}/c_{b\text{-}SNC}$ = 0.5 M/0.01 M), the internal resistance of hybrid nanochannels is increased by 49.3%, arising from the opposite direction between the salinity gradient and the preferential direction of cation transport.

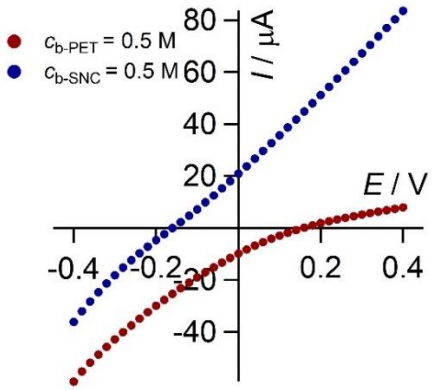

Figure S3. Measured *I-V* curves of SNC/PET hybrid nanochannels for $c_{b\text{-}SNC}$ = 0.5 M and $c_{b\text{-}PET}$ = 0.01 M (blue line) and in the concentration gradient reversed condition (red line).

As reported previously, the trans-nanochannel diffusion potential (E_{diff}) can be calculated by the following equation,[S3-S4]

$$E_{diff} = V_{oc} - E_{red} = (2t_+ - 1)\frac{RT}{F}\ln\left(\frac{c_H}{c_L}\right) \quad \text{(S1)}$$

$$\eta_{max} = \frac{(2t_+ - 1)^2}{2} \quad \text{(S2)}$$

where t_+ is the transference number of cationic ions and η the energy conversion efficiency. E_{red} is the difference of redox potentials of two Ag/AgCl electrodes. To

measure E_{red}, a home-made saturated salt bridge was used. The measured value of E_{red} is about 83.18 mV. Then t_+ can be calculated as 0.98, indicating a high cationic selectivity of SNC/PET hybrid nanochannels.

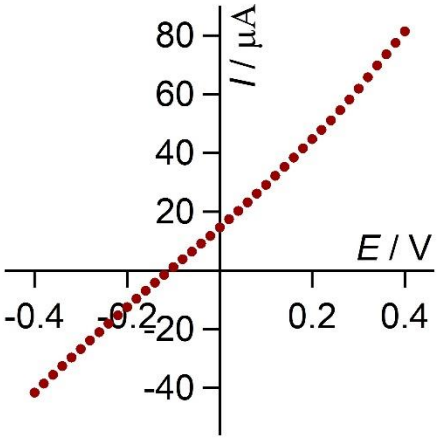

Figure S4. Measured *I-V* curve of PET conical nanochannels under a salinity gradient ($c_{b\text{-}tip}/c_{b\text{-}base}$ = 0.5 M/0.01 M NaCl).

In order to further confirm the role of SNC in energy conversion, we measured the performance of energy conversion of PET conical nanochannels. As shown in **Figure S4**, V_{oc} obtained is 106.5 mV. According to **eq. S1**, E_{diff} of PET membrane in this condition is 23.32 mV, the corresponding t_+ can be calculated as 0.62, indicating the membrane only possesses a slightly cationic selectivity. It also suggests that the highly cationic selectivity mainly originates from SNC.

S6. The Energy Conversion Performance of PET Membrane

In order to show the effect of SNC on electricity conversion, we tested the current density (j) and power density (P_R) of PET membrane under simulated seawater (0.5 M NaCl) and river water (0.01 M NaCl). As shown in **Figure S5**, j gradually decreased with the increase of R_L, the initial value is about 10.7 A m^{-2}. While P_R increased at first and then decreased after reaching a maximum, where R_L was ~20 kΩ. The maximum of P_R is about 124.6 mW m^{-2}. Compared to the performance of SNC/PET membrane (**Figure 2a**), these results demonstrate energy conversion performance is mainly dependent on SNC membrane.

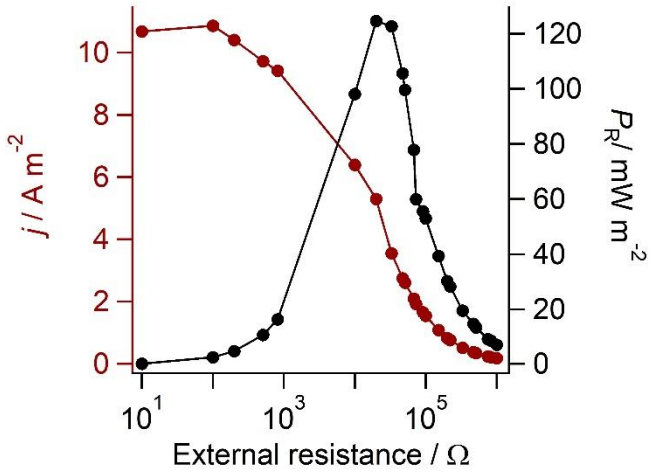

Figure S5. The current density (in red) and output power density (in black) of PET membrane as a function of the external load resistance.

S7. Numerical Simulations

Simulations of salinity gradient energy storage by SNC/PET nanochannel were carried out by the commercial finite-element software COMSOL Multiphysics 5.2. For simplicity, a 2D axis symmetric model was employed in this system, as shown in **Figure S6**.

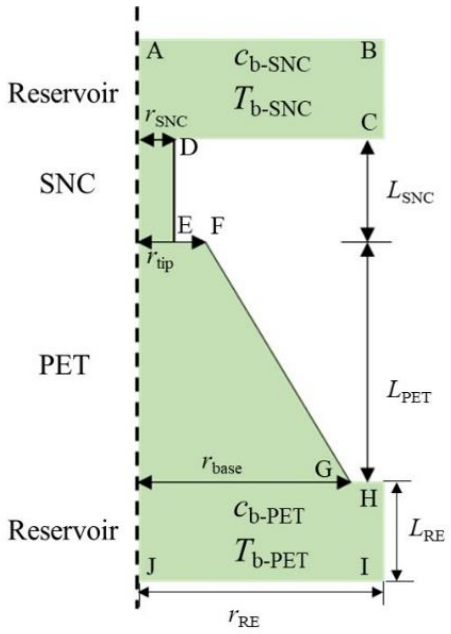

Figure S6. Scheme of 2D axial symmetric model with labeled boundaries (not to scale).

Here a conically-shaped PET channel with a tip opening radius of r_{tip} = 7 nm, a base opening radius of r_{base} = 400 nm, and a channel length of L_{PET} = 12000 nm is considered. The SNC is positioned on the side of tip, which consists of nanochannels with a radius of $r_{nanochannel}$ = 1.15 – 5 nm and a length of $L_{nanochannel}$ = 100 nm. The surface charge density of PET channel (σ_{PET}) and SNC nanochannel (σ_{SNC}) are set to be −0.002 C/m^2 and −0.015 C/m^2, respectively. This SNC/PET hybrid nanochannel is connected to two large identical reservoirs with dimensions of 100 times of r_{base}, which are filled with aqueous NaCl solutions. The boundary conditions in numerical simulation are summarized in **Table S1**.

Table S1. Boundary conditions for 2D axis symmetric model.

Boundary	Poisson equation	Nernst-Planck equation
AB	applied voltage, $\phi = V$	bulk concentration $c_+ = c_- = c_{\text{b-SNC}}$
JI	grounded, $\phi = 0$	bulk concentration $c_+ = c_- = c_{\text{b-PET}}$
BC	$-\mathbf{n}\cdot\nabla\phi = 0$	bulk concentration $c_+ = c_- = c_{\text{b-SNC}}$
HI	$-\mathbf{n}\cdot\nabla\phi = 0$	bulk concentration $c_+ = c_- = c_{\text{b-PET}}$
CD, GH	$-\mathbf{n}\cdot\nabla\phi = 0$	ion-impenetrable $\mathbf{n}\cdot\boldsymbol{j}_i = 0$
DE, EF	$-\varepsilon\mathbf{n}\cdot\nabla\phi = \sigma_{\text{SNC}}$	ion-impenetrable $\mathbf{n}\cdot\boldsymbol{j}_i = 0$
GH	$-\varepsilon\mathbf{n}\cdot\nabla\phi = \sigma_{\text{PET}}$	ion-impenetrable $\mathbf{n}\cdot\boldsymbol{j}_i = 0$

n: the unit outer normal vector.

The coupled Poisson-Nernst-Planck (PNP) and Einstein-Stokes equations are employed to quantitatively describe the ionic mass transport process,

$$\nabla^2\phi = -\frac{\rho}{\varepsilon} = -\frac{F}{\varepsilon}\sum z_i c_i \tag{S1}$$

$$j_i = -D_i\left(\nabla c_i + \frac{z_i F c_i}{RT}\nabla\phi\right) \tag{S2}$$

$$\nabla\cdot j_i = 0 \tag{S3}$$

$$D_i = \frac{k_{\text{B}}T}{6\pi\eta r} \tag{S4}$$

where

ϕ [V]: electric potential;

ρ [C/m^3]: space charge density;

$\mathbf{j}_i$ [mol/(m^2 s)]: ionic flux;

z_i [-]: charge number;

c_i [M]: ion concentration;

D_i [m^2/s]: diffusion coefficient;

ε = 78.5 [F/m]: dielectric constant of water;

F [C/mol]: Faraday constant;

R [J/K/mol]: gas constant;

k_B: Boltzmann constant;

T [K]: absolute temperature;

η [Pa*s]: the dynamic fluid viscosity of water, expressed by a built-in piecewise function in COMSOL;

r is the ion size (for Na^+, *r* = 0.4 nm; for Cl^-, *r* = 0.3 nm);[5]

i = + (for Na^+);

i = − (for Cl^-).

The model was employed to evaluate the ability of energy storage of nanochannels and the role of temperature gradient played in energy storage. We plotted the profile of energy density (U_r) along the radial direction of nanochannel before and after a temperature change of 10 K at the boundary of SNC and PET channel. The initial temperature of two solutions is set at 298.15 K ($T_{b\text{-}SNC}$ = $T_{b\text{-}PET}$ = 298.15 K). As shown in **Figure S7**, the variation of U_r in response to temperature change is too small to recognize directly. Hence, we analyzed its variation, namely ΔU_r, as shown in **Figure 4f**.

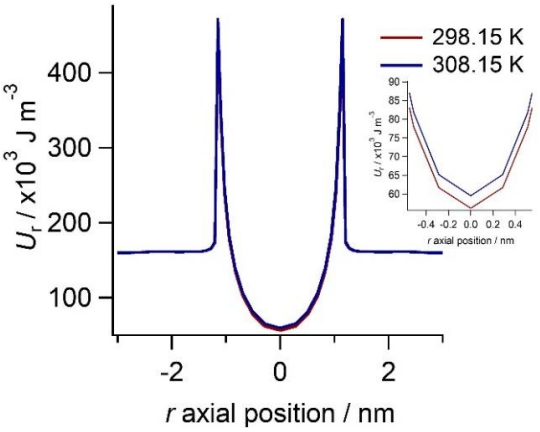

Figure S7. Calculated energy density along the radial direction of hybrid nanochannel. $c_{b\text{-}PET}$ and $c_{b\text{-}SNC}$ are set at 0.01 M and 0.5 M, respectively. $T_{b\text{-}SNC}$ and $T_{b\text{-}PET}$ are set at 298.15 K initially, then $T_{b\text{-}PET}$ is increased by 10 K to 308.15 K and $T_{b\text{-}SNC}$ is kept at 298.15 K. The inset shows the magnifications at the orifice of nanochannel.

Reference

S1 Z. Teng, G. Zheng, Y. Dou, W. Li, C.-Y. Mou, X. Zhang, A. M. Asiri, D. Zhao, *Angew. Chem. Int. Ed.* 2012, **51**, 2173.

S2 W. Wu, Q. Yang, B. Su, *J. Membr. Sci.* 2018, **558**, 86.

S3 W. Xin, Z. Zhang, X. Huang, Y. Hu, T. Zhou, C. Zhu, X.-Y. Kong, L. Jiang, L. Wen, *Nat. Commun.* 2019, **10**, 3876.

S4 F. Yan, L. Yao, K. Chen, Q. Yang, B. Su, *Journal of Materials Chemistry A* 2019, **7**, 2385.

S5 C. Duan, A. Majumdar, *Nat. Nanotechnol.* 2010, **5**, 848.